A R C H I V E O F M E C H A N I C A L E N G I N E E R I N G

VOL. LXIII 2016 Number 3

DOI: 10.1515/meceng-2016-0026

**Key words:** joined wing, performance, computational fluid dynamics, CFD

*ADAM SIERADZKI* [1], *ADAM DZIUBIŃSKI* [1], *CEZARY GALIŃSKI* [1]

# PERFORMANCE COMPARISON OF THE OPTIMIZED INVERTED JOINED WING AIRPLANE CONCEPT AND CLASSICAL CONFIGURATION AIRPLANES

The joined wing concept is an unconventional airplane configuration, known since the mid-twenties of the last century. It has several possible advantages, like reduction of the induced drag and weight due to the closed wing concept. The inverted joined wing variant is its rarely considered version, with the front wing being situated above the aft wing. The following paper presents a performance prediction of the recently optimized configuration of this airplane. Flight characteristics obtained numerically were compared with the performance of two classical configuration airplanes of similar category. Their computational fluid dynamics (CFD) models were created basing on available documentation, photographs and some inverse engineering methods. The analysis included simulations performed for a scale of 3-meter wingspan inverted joined wing demonstrator and also for real-scale manned airplanes. Therefore, the results of CFD calculations allowed us to assess the competitiveness of the presented concept, as compared to the most technologically advanced airplanes designed and manufactured to date. At the end of the paper, the areas where the inverted joined wing is better than conventional airplane were predicted and new research possibilities were described.

## 1. Introduction

The joined wing concept is an unconventional airplane configuration, known since the mid-twenties of the last century. It was proposed for the first time in 1924 by Prandtl [1], but not many of this kind of design were built since then. The joined wing configuration consists of two lifting surfaces similar in terms of area and span. One of them is located at the top or above the fuselage, whereas the second is located at the bottom. Both lifting surfaces

[1] *Institute of Aviation, Krakowska Av. 110/114, 02-256 Warsaw, Poland; Emails: Adam.Sieradzki@ilot.edu.pl, Adam.Dziubinski@ilot.edu.pl, Cezary.Galinski@ilot.edu.pl*

join each other either directly or with application of wing tip plates (box wing). The main advantages of joined wing concept are induced drag reduction and weight reduction due to the closed wing concept.

However, due to strong aerodynamic coupling [2] and static indeterminacy of the structure, creating a successful joined wing airplane design was almost impossible before CFD and FEM methods were developed. Nowadays, attempts to design a joined wing airplane are more frequent, but in most cases researchers concentrate on the primary configuration of a joined wing airplane, with the front wing below the aft wing [3–14]. The previous experience of the authors [15] led to the conclusion that the joined wing airplane could fly much better in an upside down configuration. The most probable reason for this fact comes from the interaction between the wings. CFD analysis confirmed that the newly created Inverted Joined Wing Airplane Concept (IJWAC), with the front wing located at the top of fuselage and the aft wing at the bottom, provides not only greater maximum CL/CD, but also greater CL/CD in a wider range of angles of attack [16]. The configuration with the front wing below the aft wing is advantageous only at low angles of attack, assuming that the aft wing is installed at the top of the vertical stabilizer. However, weight advantage will be reduced in this case due to increased loads of the vertical stabilizer.

The aim of the research presented in this paper is to assess the competitiveness of the last optimized version of this airplane concept with the most technologically advanced airplanes designed and manufactured to date. In the Inverted Joined Wing Scaled Demonstrator Programme [17, 18], two sessions of multicriterial aerodynamic optimization for a 3-meter wingspan UAV demonstrator have been performed so far [19]. The optimization used a Vortex Lattice Method (VLM), expanded by Prandtl equations for viscosity effects (boundary layer region), to evaluate objective functions and find optimal solutions, as it was done also in previous, similar projects [20–22]. The configuration chosen after a second optimization process from calculated Pareto-optimal solutions frontier was used in the work presented here. It is worth mentioning that the described optimization [19] was conducted for isolated lifting surfaces only (wings and wing tip plates). Other parts of the airframe (such as a fuselage, landing gear, etc.) were not included in the optimized model, but they were taken into account in part of the CFD cases presented in this paper. Therefore, this allowed one to assess their influence on the final aerodynamic characteristics of the proposed concept and compare them with classical configuration airplanes. Two simplified models of well-known high performance airplanes were created for the purposes of this study.

The created CAD/CFD models and analysis methods are described at the beginning of the paper. The information about geometry and meshes specification, simulated cases and solver settings can be found there. The CFD

simulations results are presented and discussed in the next part of the article. Finally, appropriate conclusions, based on conducted research, are drawn and possible future directions of work are proposed.

## 2. CAD models

The inverted joined wing geometry presented in this paper is the result of multicriterial aerodynamic optimization [19] performed for the scale of a 3-meter wingspan demonstrator. It was optimized to maximize the CL/CD and $CL^3/CD^2$ ratio, within the range of allowable geometry changes (constraints for front and rear wing surface, sweep, taper ratio, etc.). The final configuration, shown in Fig. 1, was optimized for an airplane weight of 25 kg and a flight speed of 24.5 m/s.

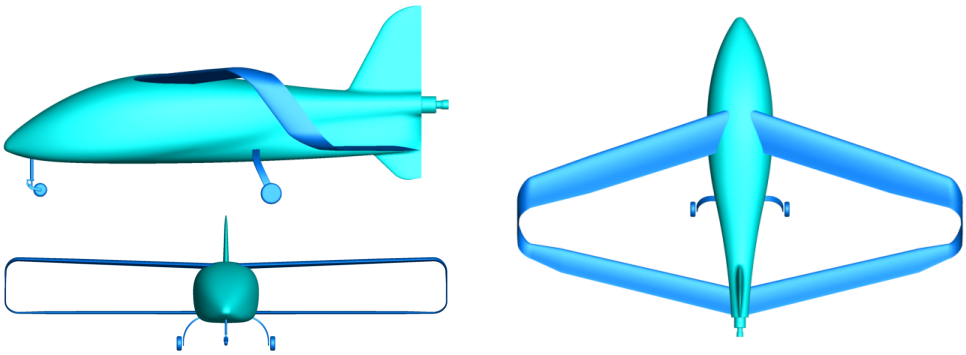

Fig. 1. Inverted joined wing complete airplane model

Two high-performance classical configuration airplanes of similar class were also modeled in order to make a comparison with the IJWAC. Due to legal reasons, the manufacturers and airplanes names could not be published and the complete models of these aircrafts could not be shown. The first of them is a two-seat high-wing ultralight airplane with fixed landing gear and T-tail configuration. Its maximum takeoff weight is about 470 kg and the cruising airspeed is about 270 km/h. The second one is a four-seat low-wing retractable-landing-gear monoplane with a classical tail configuration. With the gross weight of about 1600 kg this aircraft is able to maintain the cruising speed of more than 400 km/h. Comparing the specifications of these two planes, it is obvious that they were designed for different customers with different needs. However, they have one thing in common – distinctive aerodynamic design and performance. That is the reason for choosing them for comparison with the IJWAC in terms of aerodynamic efficiency.

The models have been created basing on available manufacturers documentation, photographs and some inverse engineering methods. The fuselages

and other non-lifting parts of the airframe were reconstructed in a free 3D polygon modeler, on the base of plans and photographs found. In turn, the lifting surfaces (wings, horizontal tails) were created directly in the CFD mesh generator software to ensure the best possible geometry representation and quality of these parts.

All CAD models for the purposes of this work were created in two scales – one corresponding to the 3-meter wingspan IJWAC demonstrator (already built and flight tested [17]) and the second corresponding to the real dimensions of the selected classical configuration airplanes. As mentioned before, each complete airplane model has two versions corresponding to two different scales. However, there were also cases where only the isolated lifting surfaces of created airplane's models were taken into account (fuselages, fins and landing gears were neglected), also for both considered scales. This approach allowed later to check the competitiveness of 'clean' lifting configurations (Figs. 2, 3), without any other parts of the airframe generating parasitic drag and interfering with the results of analyzes.

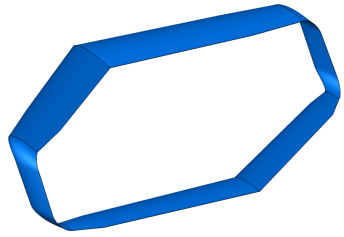

Fig. 2. Inverted joined wing isolated lifting surfaces model

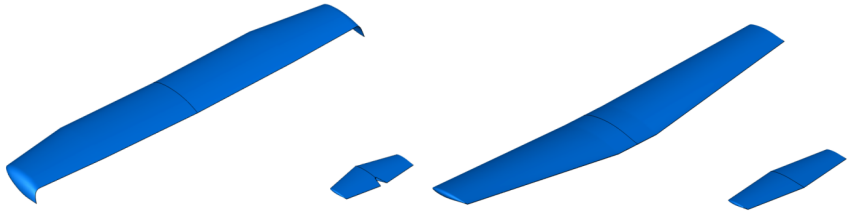

Fig. 3. First (high-wing) and second (low-wing) classical configuration isolated lifting surfaces model

In order to fairly compare two different types of airplane configuration – the classical one and the IJWAC – the total lifting surface area, including the rear wing or the horizontal tail, had to be taken into account as reference area when calculating selected aerodynamic coefficients (the data collected in Table 1).

Table 1.

Inverted joined wing complete airplane model

| Reference values: | Inverted joined wing | | High-wing monoplane | | Low-wing monoplane | |
|---|---|---|---|---|---|---|
| | scale 3:10 | scale 1:1 | scale 3:10 | scale 1:1 | scale 3:10 | scale 1:1 |
| b [m] | 3.1 | 10.3 | 3.21 | 10.7 | 3.27 | 10.9 |
| MAC [m] | 0.247 | 0.823 | 0.28 | 0.933 | 0.305 | 1.016 |
| $S_{front}$ [$m^2$] | 0.76 | 8.444 | 0.893 | 9.927 | 0.981 | 10.898 |
| $S_{rear}$ [$m^2$] | 0.5 | 5.556 | 0.098 | 1.084 | 0.176 | 1.958 |
| $S_{total}$ [$m^2$] | 1.26 | 14 | 0.991 | 11.011 | 1.157 | 12.856 |

It is important to note that the resultant models of conventional configuration airplanes are not exactly the same in terms of geometry definition as their original prototypes. These are the simplified models, created using limited information available. They should be treated rather as some example airplanes from a similar category, only based on selected existing designs, not exact copies. Therefore, the predicted aerodynamic performance of these designs could be different than the original one.

## 3. CFD analysis methods and meshes

CFD analysis, based on the Finite Volume Method (FVM), is a very useful tool in aircraft design. It combines high reliability and accuracy of results with a relatively low cost. In the following work, one of the most widely recognized as an industrial standard Reynolds-averaged Navier-Stokes (RANS) solver was used.

All the cases have been analyzed with the same solver settings and mesh parameters. A double precision pressure based solver with incompressible flow and k-ω SST Transitional (4 equations) turbulence model was used. This implied the necessity of high resolution meshes generation with y+ values around 1 and below. Tetrahedral meshes with prism layers to simulate flow in a boundary layer region were created in solver specific discretization software. So configured and prepared grids had the capability of capturing not only turbulent flow in the computational domain, but also laminar regions which potentially could have great influence on aerodynamic performance (laminar separation bubbles, etc.) in the corresponding range of Reynolds number (from about $5 \cdot 10^5$ for 3:10 scale to $3 \cdot 10^6$ for 1:1 scale). Surface roughness was not modeled, which corresponded to the assumption of perfectly smooth wetted surfaces of all calculated models.

The following boundary conditions were used in all the prepared meshes (presented in Fig. 4):

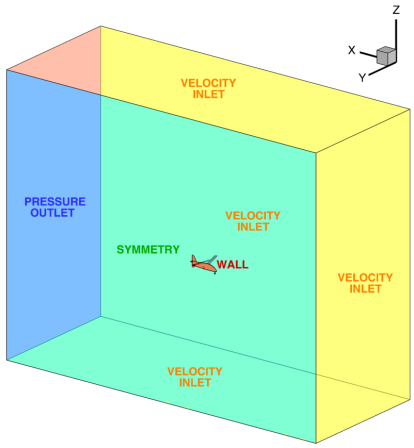


Fig. 4. An example of a computational domain with assumed boundary conditions

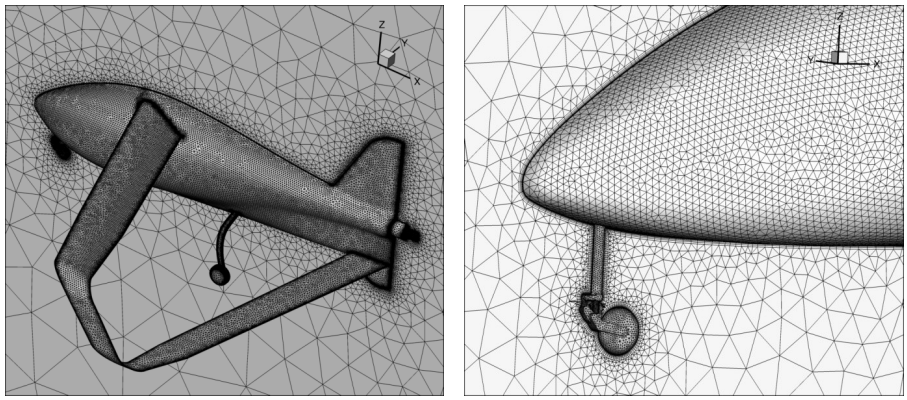

Fig. 5. An example of a computational mesh (IJWAC)

- Velocity Inlet – for inlet surfaces of the computational domain,
- Pressure Outlet – for outlet surfaces of the computational domain,
- Symmetry – for surfaces which act like symmetry planes (only half-models were analyzed),
- Wall – for all airplane surfaces.

The size of domains used in following work was:

- for 3:10 scale: 25 × 10 × 20 m
- for 1:1 scale: 83.3 × 33.3 × 66.6 m

All the configuration cases were calculated for a specified range of angle of attack with a 2 degree step. The simulation airspeed was set to 24.5 m/s for scale 3:10 (a value obtained as the result of inverted joined wing optimization) and 32 m/s for scale 1:1. The second value was obtained from the lift force equation and the assumption of the same CL:

$$mg = \frac{1}{2}\rho S C_L V^2 \leftrightarrow \frac{m}{SV^2} = \frac{\rho C_L}{2g} = \text{const} \leftrightarrow \left(\frac{m}{SV^2}\right)_{SCALE\ 3:10} = \left(\frac{m}{SV^2}\right)_{SCALE\ 1:1} \tag{1}$$

After the substitution of appropriate data of the first classical configuration airplane (ultralight high-wing monoplane) and the assumption of 25 kg mass for the 3:10 scale demonstrator, it was possible to designate the airspeed value for the real-scale:

$$\left(\frac{25\ [\text{kg}]}{0.991\ [\text{m}^2] \cdot 24.5^2\ \left[\frac{\text{m}}{\text{s}}\right]}\right)_{SCALE\ 3:10} = \left(\frac{470\ [\text{kg}]}{11.011\ [\text{m}^2] \cdot V^2\ \left[\frac{\text{m}}{\text{s}}\right]}\right)_{SCALE\ 1:1} \rightarrow \rightarrow\ V \approx 32\ \left[\frac{\text{m}}{\text{s}}\right] \tag{2}$$

The values of turbulent parameters in the external boundary conditions (Velocity Inlet and Pressure Outlet) were set as follows:

- intermittency = 1 (which corresponds to the assumption of fully turbulent flow),
- turbulence intensity = 0.1% (small value, typical for external flows [23]),
- turbulent viscosity ratio = 1 (small value, typical for external flows [23]).

The main difference in the models generated for different scales was, despite clear rescaling effects, the distinct boundary layer mesh generation. As mentioned before, prism layers were used to model the region of the boundary layer, parameters of which depend on geometrical dimensions and flow and fluid properties. Therefore, the number of layers, the height of first layer and the total height, needed to properly capture all flow phenomena with the chosen turbulence model, had to be different for both analyzed scales. The prism layers parameters were determined on the basis of the Schlichting approximation formula for turbulent boundary layer thickness and skin friction coefficient [24], and can be found in Table 2.

The number of cells in the prepared meshes varied from about 2 million – for simple isolated lifting surfaces models, to over 6 million – for much more sophisticated complete airplanes models. All meshes were created using smooth Delaunay triangulation method for tetrahedral elements (recommended for CFD meshes).

Table 2.

Prism layers parameters for both scales analyzed

| **Prism layers parameters:** | **SCALE 3:10** | **SCALE 1:1** |
|---|---|---|
| Initial height [mm] | 0.01 | 0.01 |
| Number of layers | 16 | 19 |
| Height ratio | 1.44 | 1.43 |
| Total height [mm] | 7.746 | 20.77 |

## 4. Results

The presented models of isolated lifting surfaces (wings) and of complete airplanes were compared primarily for glide ratio (CL/CD) and endurance factor ($CL^3/CD^2$). These two aerodynamic performance indicators give information about the potential of the selected configuration, in terms of flight range and endurance. Moreover, the dimensionless glide ratio value is independent of the assumed reference values and therefore, fraught with the smallest methodical error. On the other hand, the value of the endurance factor for the selected airplane changes when the assumed reference area value is modified. This is the reason for using the total lifting surface area as a reference area in all calculated cases.

All 3:10 scale wing configurations were trimmed only once at the beginning of simulations, for a CL value of about 0.3, using XFLR5 software for this purpose. Both CL ≈ 0.3 (in Fig. 6) and Cm ≈ 0 (in Fig. 7) for the selected configuration are achieved at the same angle of attack. During later CFD analysis the longitudinal balance was not provided.

In Fig. 8 it can be seen that the tested lifting surfaces configurations are similar in terms of maximum glide ratio value, especially in 1:1 scale. For

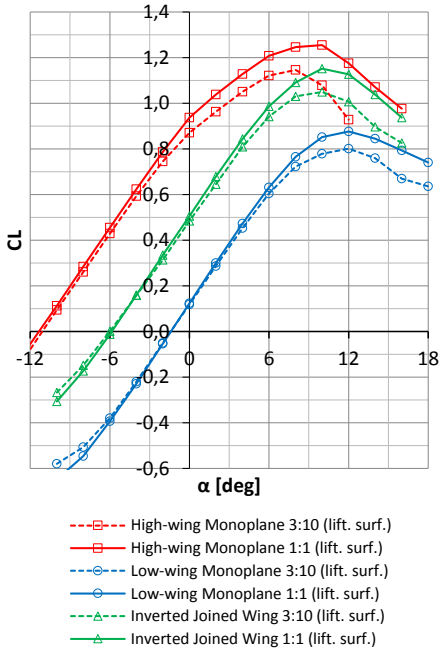


Fig. 6. CL(α) curves for all lifting surfaces models

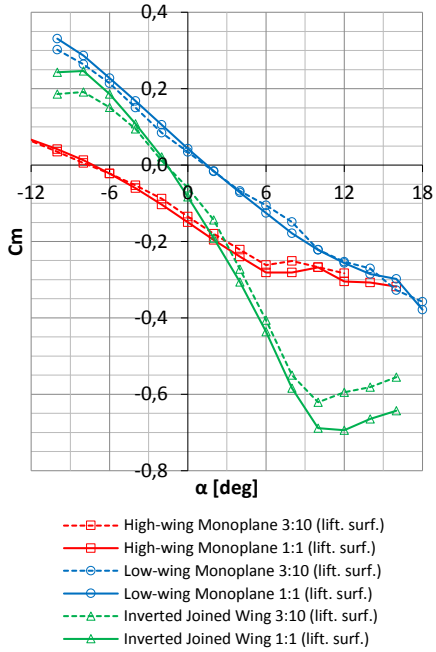


Fig. 7. Cm(α) curves for all lifting surfaces models

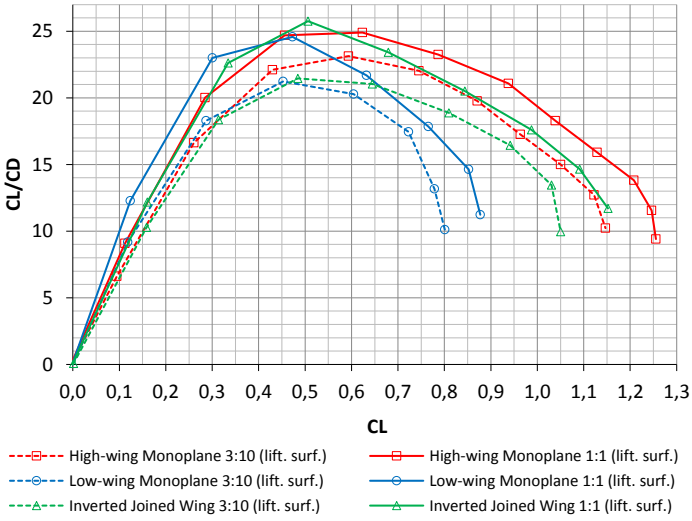


Fig. 8. CL/CD ratio vs. CL for all isolated lifting surfaces models

3:10 scale the ultralight high-wing monoplane model turned out to be about 8% better than the two other airplanes, but for real-scale and in a small range of CL it was slightly outperformed by the IJWAC (the only configuration with maximum CL/CD over 25). When taking into account Fig. 9, it is clearly visible that the ultralight high-wing monoplane dominates in endurance factor comparison for both scales and the IJWAC is about 12–20% worse, but better than the second classical configuration airplane (low-wing monoplane).

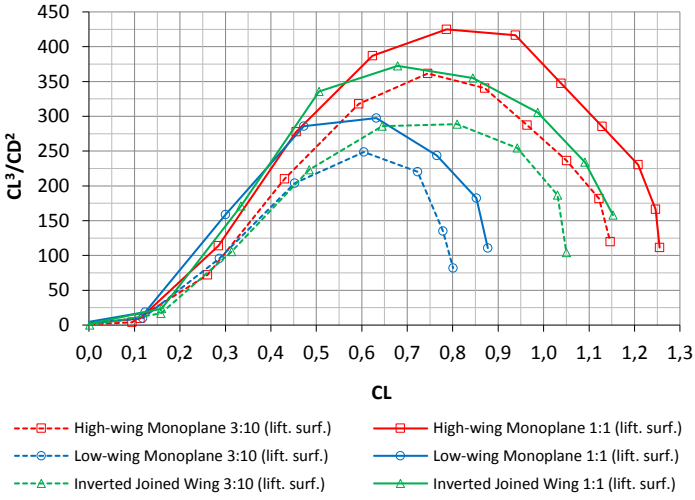


Fig. 9. $CL^3/CD^2$ ratio vs. CL for all isolated lifting surfaces models

For the complete airplanes models, the situation appears to be quite different (Figs. 10, 11). The IJWAC has the lowest maximum value of the glide ratio of all the simulated airplanes, in both scales. It is about 15% lower for 3:10 scale and 11% lower for 1:1 scale, compared to the best conventional configuration airplane. Also, the endurance factor for the complete inverted joined wing airplane is not as high as could be expected when taking into account Fig. 9.

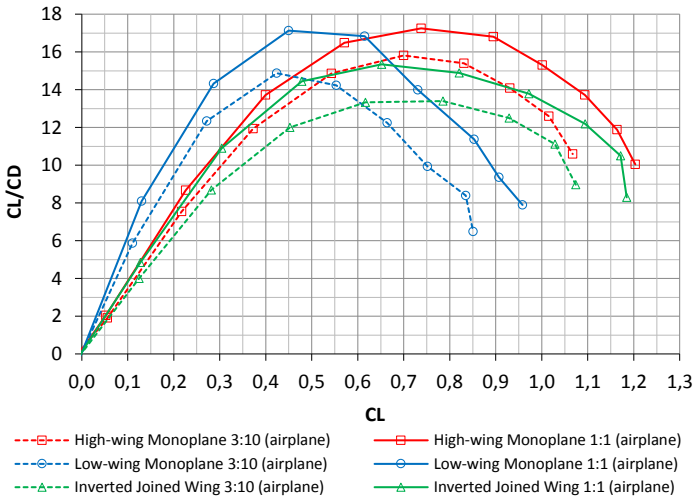


Fig. 10. CL/CD ratio vs. CL for all complete airplanes models

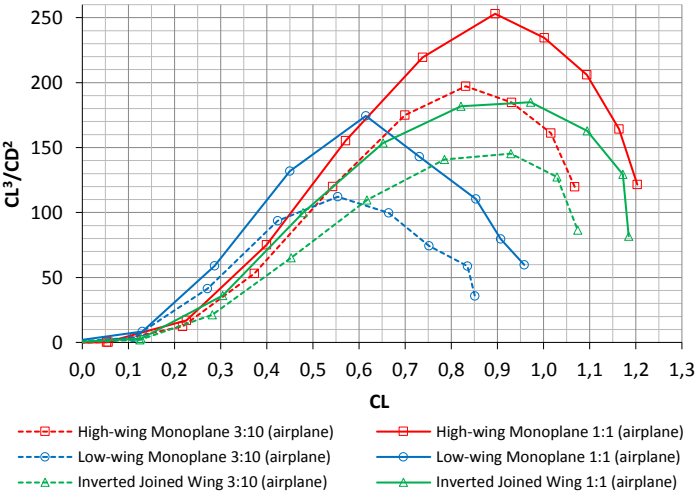


Fig. 11. $CL^3/CD^2$ ratio vs. CL for all complete airplanes models

## 5. Discussion

For the purposes of this work, the IJWAC was compared with two classical configuration airplanes in two scales: 1:1 and 3:10. The first comparison, related to isolated lifting surface models, showed a very good competitiveness of the presented joined wing configuration, especially in real-scale conditions. It also turned out that the proposed concept has the biggest aerodynamic performance improvement (20–30%) when comparing the two analyzed scales (Table 3). The reason for this is the largest wetted surface area ($S_{WET}$) of the

Table 3.
Aerodynamic efficiency indicators comparison for all isolated lifting surfaces models (both scales)

| **Isolated lifting surfaces model:** | **$S_{WET}$ [m$^2$] (scale1:1)** | **$(CL/CD)_{max}$** | | | **$(CL^3/CD^2)_{max}$** | | |
|---|---|---|---|---|---|---|---|
| | | **scale 3:10** | **scale 1:1** | **$\Delta_{scales}$ [%]** | **scale 3:10** | **scale 1:1** | **$\Delta_{scales}$ [%]** |
| High-wing monoplane | 22.7 | 23.1 | 24.9 | +7.6 | 361.5 | 424.9 | +17.5 |
| Low-wing monoplane | 26.6 | 21.2 | 24.6 | +15.8 | 248.5 | 297.6 | +19.8 |
| Inverted joined wing | 30.9 | 21.5 | 25.8 | +20 | 288.6 | 372.5 | +29.1 |

IJWAC and the change of airflow nature connected with scale change. The CFD results showed that in 3:10 scale the viscosity effects play a much greater role and that the laminar separation bubbles form along the entire front and rear wing (Fig. 12). This results in an increase of aerodynamic drag. For the larger 1:1 scale this phenomenon does not occur. Both classical configuration airplanes also suffer from this issue, but their aerodynamic performance deterioration is lower, because of a smaller wetted area. Therefore, it could be stated that the IJWAC is better suited for real-scale (manned or UAV) airplanes, which operate at high Reynolds numbers, than for small UAVs. Higher Reynolds

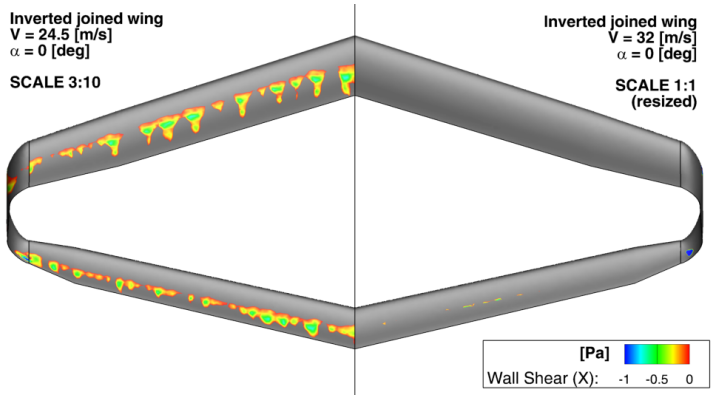


Fig. 12. Reversed flow regions for inverted joined wing lifting surfaces model (both scales compared)

number means less significant viscosity effects, thus a smaller wetted-surface-dependent aerodynamic drag value associated with them. Then, induced drag plays a more important role, which is minimized in the IJWAC due to the closed wing configuration. Moreover, the advantage of the IJWAC over conventional airplanes in real-scale should be even higher if its aerodynamic optimization process would be performed directly for real-scale conditions. It should be recalled that the configuration compared here was optimized only for 3:10 scale and then resized, which certainly did not allow to achieve maximum possible performance for this scale.

On the other hand, when comparing complete airplanes models, it turned out that both classical configuration airplanes have some advantage over the IJWAC. As expected, the second model of a much heavier and faster low-wing monoplane has better CL/CD ratio in the low CL range and lower zero-lift CD (Fig. 13), mainly due to retractable landing gear and a smoother fuselage. Whereas, the first model, based on an ultralight high-wing airplane, turned out to be better than IJWAC in both CL/CD ratio and $CL^3/CD^2$ in the whole range of usable CL.

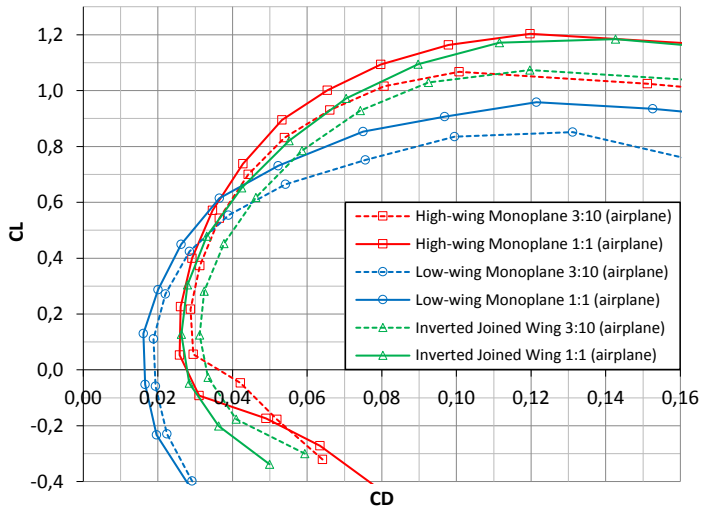


Fig. 13. CL(CD) curves (polars) for complete airplanes models

The reason for such a reduction of the complete inverted joined wing airplane competitiveness could be found in a thorough aerodynamic drag analysis (Figs. 14, 15). The figures demonstrate a greater participation of the non-lifting components of the airframe (fuselage with vertical tail, landing gear) in the generation of aerodynamic drag for the IJWAC, compared to the high-wing monoplane. This problem is clearly visible in both analyzed scales. However,

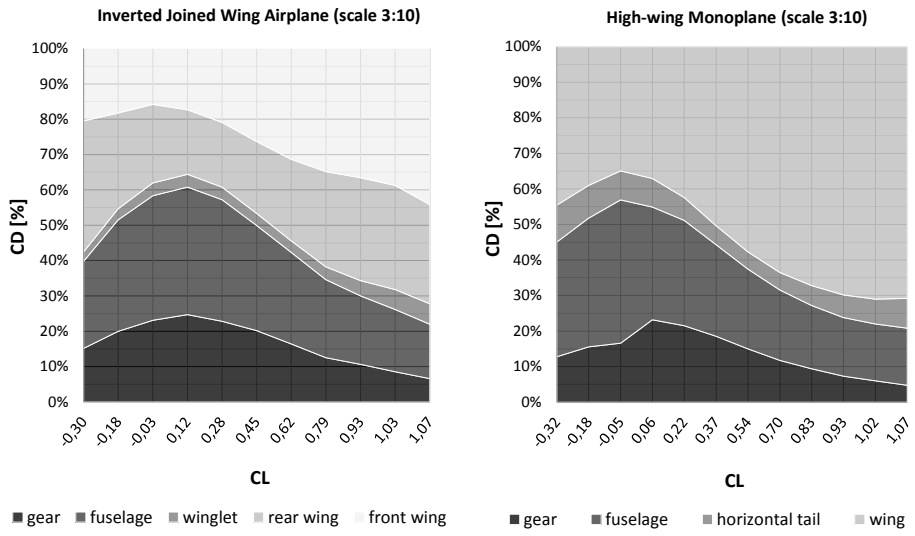


Fig. 14. The share of individual airframe parts in aerodynamic drag generation for inverted joined wing and ultralight high-wing monoplane – complete airplanes models (scale 3:10)

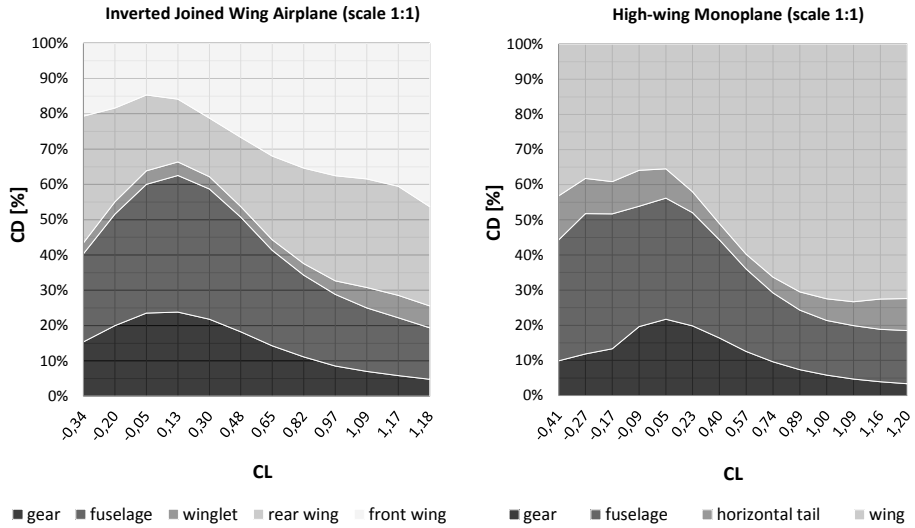


Fig. 15. The share of individual airframe parts in aerodynamic drag generation for inverted joined wing and ultralight high-wing monoplane – complete airplanes models (scale 1:1)

the fuselage used in the IJWAC model (shown in Fig. 1) was designed mainly on the base of utility requirements and is more spacious compared to the fuselages of two other airplanes. It has not been optimized in terms of aerodynamic efficiency yet, which gives an opportunity for further performance improvement (fuselage and interference drag reduction). On the other hand,

the geometries of the two classical configuration airplane's fuselages were based on real geometries (drawings, photographs) and certainly their original sources have been very well optimized. Also, the landing gear in the considered high-wing monoplane creates less parasitic drag due to well-designed wheel fairings. Such fairings were not present in the actual inverted joined wing complete airplane model.

## 6. Conclusions

In this paper, the Inverted Joined Wing Airplane Concept (IJWAC) was compared with two high-performance conventional airplanes of similar application. The computational fluid dynamics calculations were performed for two scales: the scale of a 3-meter unmanned demonstrator and the real-scale of selected airplanes. The results for the isolated lifting surfaces models showed that the optimized IJWAC could achieve comparable flight performance characteristics (glide ratio) to very well designed conventional airplanes, especially in real-scale conditions. However, this is only possible in a relatively narrow range of lift coefficients (CL). For this reason the presented IJWAC cannot be treated as a competitive candidate for a highly maneuverable airplane, which has to operate in a wide CL range. Nevertheless, taking into account precisely defined cruise conditions (CL $\approx$ 0.5) the optimized lifting surface model of IJWAC is in fact slightly better than both classical configurations in the real-scale. This indicates that the IJWAC could be better suited for long haul flights, when the flight conditions remain constant most of the time. Unfortunately, the potential of the optimized lifting surface model of the presented IJWAC was actually wasted by the relatively high parasitic drag of other prototype parts of the airframe, or the interference effects. The payload space of the model scale demonstrator could have been oversized too. The fuselage or landing gear also require precise aerodynamic optimization to minimize parasitic drag and make the complete airplane, not only its isolated lifting surface model, truly competitive. Real-scale multicriterial aerodynamic optimization of lifting surfaces and other airframe parts could allow the designing of an inverted joined wing airplane, which would outperform the most technologically advanced manned conventional airplanes built so far.

## Acknowledgements

This work was supported by The National Centre for Research and Development under grant No. PBS1/A6/14/2012.

Manuscript received by Editorial Board, November 08, 2015;
final version, July 05, 2016.

## References


[1] L. Prandtl. *Induced drag of multiplanes*. NACA TN 182, 1924.

[2] Z. Goraj, P. Kulicki, and M. Lasek. Aircraft stability analysis for strongly coupled aerodynamic configuration. *Journal of Theoretical and Applied Mechanics*, 35(1):137–158, 1997.

[3] J. Wolkovitch. The joined wing – an overview. *Journal of Aircraft*, 23(3):161–178, 1986.

[4] S. Danilecki. Zamknięte skrzydło – zalety i wady (I). (The joined wing – advantages and disadvantages (I)). *Technika Lotnicza i Astronautyczna (Aviation and Astronautics Technique)*, 9:4–6, 1988 (in Polish).

[5] S. Danilecki. Zamknięte skrzydło – zalety i wady (II). (The joined wing – advantages and disadvantages (II)). *Technika Lotnicza i Astronautyczna (Aviation and Astronautics Technique)*, 10:8–10, 1988 (in Polish).

[6] I. Kroo, S. Smith, and J. Gallman. Aerodynamic and structural studies of joined-wing aircraft. *Journal of Aircraft*, 28(1):74–81, 1991.

[7] J.E. Burkhalter, D.J. Spring, and M.K. Key. Downwash for joined-wing airframe with control surface deflections. *Journal of Aircraft*, 29(3):458–464, 1992.

[8] J.W. Gallman, S.C. Smith, and I.M. Kroo. Optimization of joined-wing aircraft. *Journal of Aircraft*, 30(6):897–905, 1993.

[9] M. Blair, R.A. Canfield, and R.W. Roberts. Joined-wing aeroelastic design with geometric nonlinearity. *Journal of Aircraft*, 42(4):832–848, 2005.

[10] C.C. Rasmussen, R.A. Canfield, and M. Blair. Joined-wing sensor-craft configuration design. *Journal of Aircraft*, 43(5):1470–1478, 2006.

[11] V.L. Bond, R.A. Canfield, M. da Luz Madruga Santos Matos, A. Suleman, and M. Blair. Joined-wing wind-tunnel test for longitudinal control via aftwing twist. *Journal of Aircraft*, 47(5):1481–1489, 2010.

[12] P.W. Jansen, R.E. Perez, and J.R.R.A. Martins. Aerostructural optimization of nonplanar lifting surfaces. *Journal of Aircraft*, 47(5):1490–1503, 2010.

[13] N. Paletta, M. Belardo, and M. Pecora. Load alleviation on a joined-wing unmanned aircraft. *Journal of Aircraft*, 47(6):2005–2016, 2010.

[14] G. Bindolino, G. Ghiringhelli, S. Ricci, and M. Terraneo. Multilevel structural optimization for preliminary wing-box weight estimation. *Journal of Aircraft*, 47(2):475–489, 2010.

[15] C. Galinski. Results of testing of models of joint-wing utility class aircraft. *SAE Aerospace Atlantic Conference*, Dayton, Ohio, 7-10 April, 1992. Paper No. 921013.

[16] P. Mamla and C. Galinski. Basic induced drag study of the joined-wing aircraft. *Journal of Aircraft*, 46(4):1438–1440, 2009.

[17] C. Galinski, J. Hajduk, A. Dziubinski, and A. Sieradzki. Progress in inverted joined wing scaled demonstrator programme. *5th CEAS Air&Space Conference*, Delft, 7-11 Sept., 2015.

[18] C. Galinski and J. Hajduk. Assumptions of the joined wing flying model programme. *Transactions of the Institute of Aviation*, 238(1):7–21, 2015.

[19] W. Stalewski. Aerodynamic optimization of joined-wing aeroplane. *6th International Conference on Experiments/Process/System Modelling/Simulation/Optimization*, Athens, 8-11 July, 2015.

[20] W. Stalewski. Parametric modelling of aerodynamic objects-the key to successful design and optimisation. *Aerotecnica Missili e Spazio*, 29(1/2):23–31, 2012.

[21] W. Stalewski and J. Zoltak. Optimisation of the helicopter fuselage with simulation of main and tail rotor influence. In *Proceedings of the ICAS Congress*, Brisbane, 2012. Paper 2012–1.4.1

[22] W. Stalewski and J. Zoltak. Multi-objective and multidisciplinary optimization of wing for small airplane. In *Proceedings of the CEAS Congress*, pages 1483–1492, Venice, 24-28 Oct. 2011.

[23] ANSYS: Fluent User's Guide, ANSYS 14.5 Help.

[24] H. Schlichting. *Boundary-Layer Theory*. McGraw-Hill, 7 edition, 1979.

**Porównanie osiągów zoptymalizowanego samolotu w odwróconym układzie skrzydeł połączonych z samolotami o klasycznej konfiguracji**

S t r e s z c z e n i e

Układ skrzydeł połączonych jest niekonwencjonalną konfiguracją samolotu, znaną od lat 20. ubiegłego stulecia. Cechuje go kilka istotnych zalet, takich jak redukcja oporu indukowanego oraz masy samolotu, ze względu na koncepcję zamkniętego skrzydła. Samolot w odwróconym układzie skrzydeł połączonych jest rzadko rozpatrywanym wariantem tej konfiguracji, z przednim skrzydłem usytuowanym nad skrzydłem tylnym. Niniejszy artykuł przedstawia oszacowanie osiągów zoptymalizowanej wersji tego typu samolotu. Charakterystyki aerodynamiczne, uzyskane na drodze obliczeń numerycznych CFD (Computational Fluid Dynamics – obliczeniowa mechanika płynów), zostały porównane z osiągami dwóch samolotów zbliżonej kategorii o układzie klasycznym. Ich modele obliczeniowe zostały stworzone bazując na dostępnej dokumentacji, zdjęciach oraz metodach projektowania odwrotnego. Analiza obejmowała symulacje wykonane dla skali bezzałogowego demonstratora o rozpiętości skrzydeł 3 m oraz pełnowymiarowej skali, odpowiadającej załogowym samolotom. Tym sposobem, wyniki obliczeń CFD pozwoliły ocenić konkurencyjność zaprezentowanej koncepcji, w porównaniu do najbardziej zaawansowanych technologicznie, obecnie projektowanych i budowanych, samolotów. Na końcu artykułu wskazano obszary, w których odwrócony układ skrzydeł połączonych charakteryzują potencjalnie lepsze osiągi niż układ konwencjonalny i zaproponowano dalszy możliwy kierunek prac.